

# Thermoelectric Properties of $\text{Ca}_3\text{Co}_4\text{O}_9$ -Based Ceramics Doped with Fe and/or Y

A.S. FEDOTOV<sup>a</sup>, A.K. FEDOTOV<sup>a,\*</sup>, A.V. MAZANIK<sup>a</sup>, I.A. SVITO<sup>a</sup>, A.M. SAAD<sup>b</sup>,  
I.O. TROYANCHUK<sup>c</sup>, M.V. BUSHINSKI<sup>c</sup>, V.V. FEDOTOVA<sup>c</sup>, P. ZUKOWSKI<sup>d</sup>  
AND T.N. KOLTUNOWICZ<sup>d</sup>

<sup>a</sup>Belarusian State University, Independence av. 4, 220030 Minsk, Belarus

<sup>b</sup>Al-Balqa Applied University, P.O. Box 4545, Amman 11953, Jordan

<sup>c</sup>Scientific-Practical Materials Research Center of NASB, 220072 Minsk, Belarus

<sup>d</sup>Department of Electrical Devices and High Voltages Technologies, Lublin University of Technology  
Nadbystrzycka 38a, 20-618 Lublin, Poland

We describe here structure and temperature dependences of conductivity  $\sigma(T)$ , the Seebeck coefficient  $\alpha(T)$ , thermal conductivity  $\lambda(T)$  and figure-of-merit  $ZT(T)$  in  $\text{Ca}_3\text{Co}_4\text{O}_9$  ceramics, doped with Fe and Y, depending on compacting pressure (0.2 or 6 MPa) and temperature ( $300 < T < 700$  K). It is shown that introduction of iron and yttrium to ceramics does not alter the crystalline structure of the material. Increasing the pressure in the compacting process before the additional diffusion annealing leads to a smaller-grained structure and increase  $\sigma$  and  $\lambda$  due to reducing of the synthesized samples porosity. The Seebeck coefficients of nanocomposite ceramics  $\text{Ca}_3\text{Co}_{3.9}\text{Fe}_{0.1}\text{O}_9$  and  $(\text{Ca}_{2.9}\text{Y}_{0.1})(\text{Co}_{3.9}\text{Fe}_{0.1})\text{O}_9$  have linear dependences on temperature is not changed after increase of compacting pressure. Electrical-to-heat conductivity ratio ( $\sigma/\lambda$ ) for the samples compacted at high (6 GPa) pressure increases not more than 20–30% in comparison with ones compacted at low (0.2 GPa) pressure, whereby  $ZT$  is increased more than 50%. The main reason for this effect is samples porosity reduction with the compacting pressure increase.

DOI: [10.12693/APhysPolA.125.1344](https://doi.org/10.12693/APhysPolA.125.1344)

PACS: 46.25.Hf, 62.20.D–, 82.45.Xy

## 1. Introduction

A lot of attention because of the need to find a cleaner way of converting harvesting heat into electricity was drawn to the solid-state thermoelectric converters that use the Seebeck, Peltier, and Thomson effects. The thermoelectric generators (TEG) have a number of advantages over traditional electric generators because of the relative simplicity of the design, the lack of moving parts, noiseless operation, high reliability, miniaturization without loss of efficiency, etc. However, for wide industrial applications TEG have to significantly increase their figure-of-merit. This is especially important for “long-range space” applications, which require not only increase the efficiency of TEG, but also reduced their weight/size characteristics.

One of the most famous and popular today thermoelectric materials (TEM) are compound semiconductors based on bismuth telluride and lead. However, this type of materials has a number of disadvantages: their toxicity, low content of their components in the Earth crust, low thermal stability (e.g., the melting point of bismuth telluride is 835 K) although possessing  $ZT \approx 1$ . Therefore, attempts are being made to find new and improved

properties of the known and new TEMs which can work at higher temperatures. One of the mostly studied classes of new TEMs include such oxides as sodium and calcium cobaltites, strontium titanates, zinc and manganese oxides, etc. [1–5]. Their advantages are apparent ability to operate at high temperatures (at least up to 1300 K), unreactiveness and, as a result, environmental friendliness, accessibility and relative cheapness of their constituent elements.

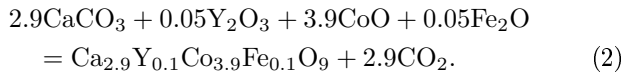
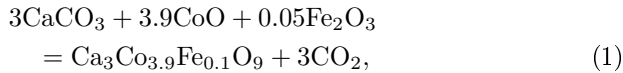
The aim of this study is to investigate basic parameters of thermoelectric (Seebeck coefficient, conductivity, heat conductivity and thermoelectric figure-of-merit) of oxide ceramics such as doped calcium cobaltites like  $\text{Ca}_3\text{Co}_{3.9}\text{Fe}_{0.1}\text{O}_9$  and  $(\text{Ca}_{2.9}\text{Y}_{0.1})(\text{Co}_{3.9}\text{Fe}_{0.1})\text{O}_9$ , using Harman method. Studying the effect of doping and synthesis regimes on the structure and thermoelectric properties of the samples allowed to describe, on a qualitative level, the factors affecting the  $ZT$  of the investigated cobaltites, and to analyze the possible approaches to its increase.

## 2. Experimental

Polycrystalline samples  $\text{Ca}_3\text{Co}_{3.9}\text{Fe}_{0.1}\text{O}_9$  and  $(\text{Ca}_{2.9}\text{Y}_{0.1})(\text{Co}_{3.9}\text{Fe}_{0.1})\text{O}_9$  were synthesized by a standard ceramic technology using oxides  $\text{Y}_2\text{O}_3$ ,  $\text{Fe}_2\text{O}_3$ , and carbonates  $\text{CaCO}_3$  (all materials qualification OFS) as starting reagents. Oxides of rare earth elements were previously annealed in air at 1000°C for 2 h to

\*corresponding author; e-mail: [fedotov@bsu.by](mailto:fedotov@bsu.by)

lower moisture. The calculation of initial components performed according to the following chemical reactions:



Taken in the desired stoichiometric ratio, the oxide powders were milled with a small amount of ethyl alcohol in an automatic RETSCH planetary mill to obtain a homogeneous particulate state. The resulting powder was packed into a steel cylindrical mold of 20 mm diameter and subjected to pressing of tablet-like samples at room temperature with an automatic hydraulic press. The pressure was 0.2 GPa and the exposure time in the loaded state of about 15–20 s. To exclude the samples inhomogeneity, effort removal after pressing occurred with a rate of 0.02 GPa/s. Preliminary heat treatment of powder mixtures for synthesis of the material was performed in air at temperatures of 1230–1270 K for 2 h. Further, the resulting material was re-milled and re-pressed at room temperature under pressure 0.2 GPa for the final synthesis. The synthesis was carried out on a platinum substrate in air furnace with molybdenum disilicide-heaters, the temperature of which was controlled by a Pt/Pt–6%Rh thermocouple. Setting the rate of heating and cooling of the samples was carried out using a special PID controlling system.

The final synthesis was carried out at 920 °C for 15 h. Cooling rate after synthesis can be varied from 20 to 2000 °C/h. Samples re-milled into powder again after synthesis, compacted at room temperature into tablets under pressures either 0.2 GPa or 6 GPa and then subjected to diffusion annealing at 750 °C for 2 h for the samples homogenization. The oxygen presence in the synthesized samples was determined by thermogravimetric analysis by weight loss on reduction to simple oxides. Deviation was not more than 0.2% of the total oxygen content in the samples. It was found that the oxygen content in the samples may vary in a wide range. In this case, the introduction of Fe led to a deficiency of oxygen.

The synthesized samples were preliminarily subjected to the study of structure and chemical composition using scanning electron microscope LEO 1455VP microscope and X-ray diffractometer DRON-4 for XRD analysis. LEO 1455VP was equipped with a special microprobe X-ray analyzer with energy-dispersive Si:Li detector Rontec allowing to perform X-ray microanalysis for checking the samples' stoichiometry with accuracy of  $\approx 1\%$ . For the thermoelectric characterization we used an automated measuring system (AMS), which allowed to study temperature dependences of thermoelectric figure-of-merit  $ZT(T)$ , Seebeck coefficient  $\alpha(T)$  and electrical conductivity  $\sigma(T)$  by the Harman method [6]. The main technical characteristics of the AMS were the following:

- determination of the  $\sigma(T)$  range —  $10^{-5}$ – $10^3 \Omega \text{ cm}$  with the accuracy not less than 10%;

- determination of the  $\alpha(T)$  range — 10–1000  $\mu\text{V/K}$  with the accuracy not less than 0.5%;
- determination of  $ZT(T)$  range with the accuracy not less than 5%;
- determination of  $\lambda(T)$  range — 0.5–10  $\text{W}/(\text{m K})$  with the accuracy not less than 15%;
- measurement of temperature with the error not more than 0.1 °C in the range 300–700 K;
- measurement error of voltage by nanovoltmeter Agilent 34420A (at the limit of measurement 100 mV) — no more than 0.0002% of measured value  $+0.1 \mu\text{V}$ ;
- current measurement error — no more than 0.15%;
- stabilization of the temperature range 300–700 K with an accuracy of 1%;
- vacuum level in the measuring chamber — 1 Pa.

After measurements of  $ZT(T)$ ,  $\alpha(T)$ , and  $\sigma(T)$  dependences we could estimate  $\lambda(T)$  with accuracy not less than 15% using the known Ioffe relation for dimensionless  $ZT = \alpha^2 \sigma T / \lambda$  [7].

Measurements of  $\sigma(T)$  at  $50 < T < 300$  K were performed in the closed-cycle cryogen-free cryostat system (Cryogenic Ltd., London). The PC based control system with Lakeshore Temperature Controller (Model 331) allowed to scan the temperature with a rate of about 0.1–1 K/min and to stabilize it (if necessary) with accuracy 0.005 K. The relative error of conductance measurements was less than 0.1%.

### 3. Results and discussion

According to XRD analysis, the introduction of iron and yttrium into  $\text{Ca}_3\text{Co}_4\text{O}_9$ -based ceramics did not lead to the appearance of new phases. As can be seen from insets in Fig. 1, the X-ray patterns of the synthesized samples, subjected to low (0.2 GPa) and high (6 GPa) compaction pressure before final diffusion heat treatment, have no qualitative differences.

Example of SEM images for the ceramic samples  $\text{Ca}_3\text{Co}_{3.9}\text{Fe}_{0.1}\text{O}_9$ , obtained by compaction at low (0.2 GPa) and high (6 GPa) pressures, prior to final homogenizing heat treatments, are presented in Fig. 1. It is evident that increasing the compacting pressure leads to a finer-grained structure and also reduces the porosity of the synthesized samples of both groups.

The example of  $ZT(T)$ ,  $\alpha(T)$ ,  $\sigma(T)$  and calculated  $\lambda(T)$  dependences for the samples  $\text{Ca}_3\text{Co}_{3.9}\text{Fe}_{0.1}\text{O}_9$  is presented in Fig. 2. Let us compare the behavior of these dependences for both groups of cobaltites doped with iron only (samples 1 compacted at 0.2 GPa and samples 2 for 6 GPa) or doped with iron and yttrium simultaneously (samples 3 compacted at 6 GPa).

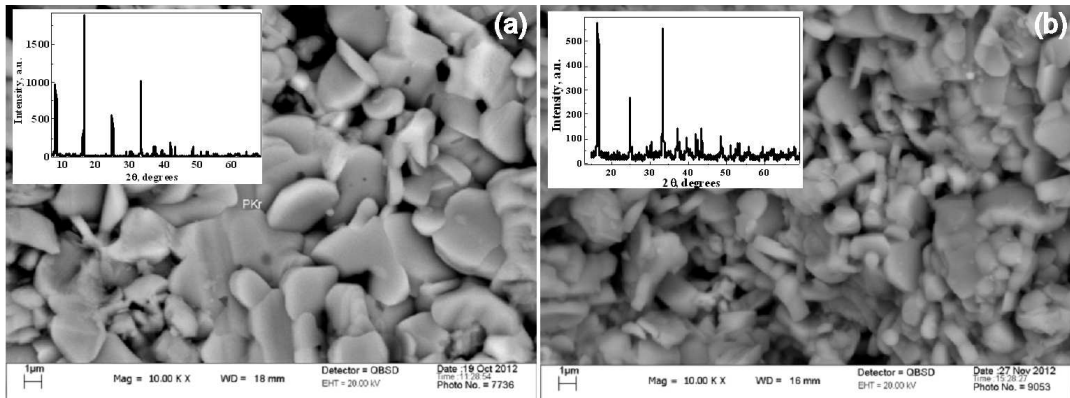


Fig. 1. SEM images and XRD patterns in insets for the ceramic samples  $\text{Ca}_3\text{Co}_{3.9}\text{Fe}_{0.1}\text{O}_9$  after compaction at pressures 0.2 GPa (a) and 6 GPa (b) before homogenization heat treatment.

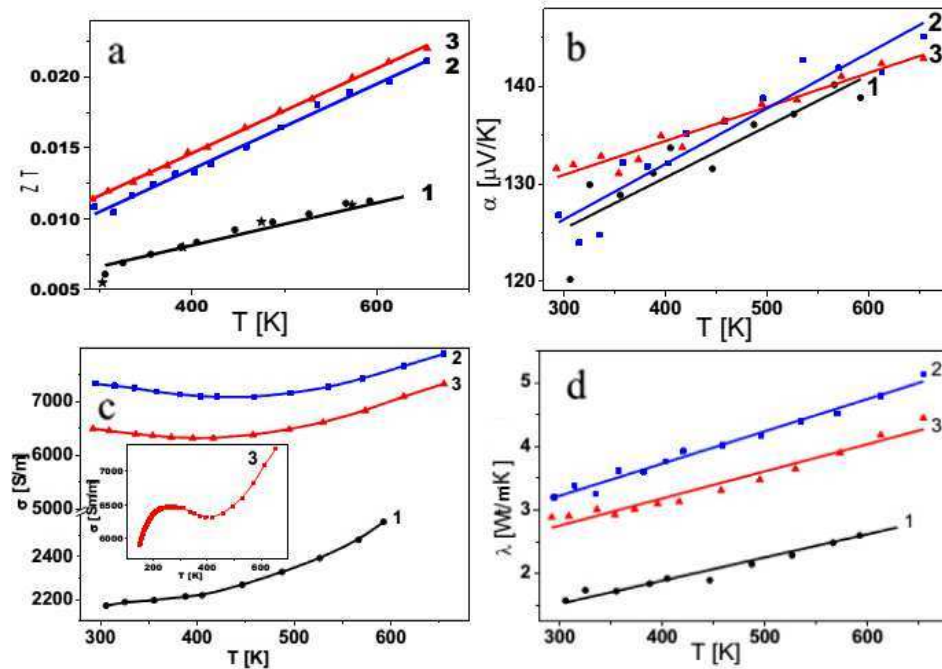


Fig. 2. Temperature dependences of thermoelectric parameters  $ZT$  (a),  $\alpha$  (b),  $\sigma$  (c) and  $\lambda$  (d) of the ceramic samples  $\text{Ca}_3\text{Co}_{3.9}\text{Fe}_{0.1}\text{O}_9$  (curves 1 and 2) and  $(\text{Ca}_{2.9}\text{Y}_{0.1})(\text{Co}_{3.9}\text{Fe}_{0.1})\text{O}_9$  (curves 3) after compaction at pressures 0.2 GPa (curves 1) and 6 GPa (curves 2 and 3) before homogenization heat treatment. Inset:  $\sigma(T)$  for  $(\text{Ca}_{2.9}\text{Y}_{0.1})(\text{Co}_{3.9}\text{Fe}_{0.1})\text{O}_9$  sample measured in the temperature range 2–700 K.

Firstly, we should note that there were no difference in  $ZT(T)$ ,  $\alpha(T)$ ,  $\sigma(T)$  and  $\lambda(T)$  dependences between the samples with different doping subjected low pressure 0.2 GPa at compaction of tablets before homogenization annealing. It is clearly seen, for example, in the curve 1 in Fig. 1a where two different types of points conform  $\text{Ca}_3\text{Co}_{3.9}\text{Fe}_{0.1}\text{O}_9$  (diamonds) and  $(\text{Ca}_{2.9}\text{Y}_{0.1})(\text{Co}_{3.9}\text{Fe}_{0.1})\text{O}_9$  (stars) samples.

Secondly, the analysis of the experimental data for the both groups of samples have shown that the increase of

compaction pressure (from 0.2 GPa to 6 GPa) before homogenization annealing is mostly critical factor which strongly affects properties of the samples studied. As is seen, higher pressure of compaction results in increase of conductivity in 2–4 times and thermal conductivity and figure-of-merit in 2–3 times whereas Zeebeck effect  $\alpha(T)$  remains practically invariable (compare curves 1 and 2–3 in Fig. 1), hitting in narrow band of values between 120–130  $\mu\text{V}/\text{K}$  at 300 K and 140–145  $\mu\text{V}/\text{K}$  at 700 K (see Fig. 1b).

Thirdly, as is seen from Fig. 2a,b,d,  $ZT(T)$ ,  $\alpha(T)$ , and  $\lambda(T)$  dependences are close to linear independently on compaction pressure. At the same time,  $\sigma(T)$  curves in Fig. 2c are non-linear and even non-monotonic (see curve 3 in the inset) in the wide range of temperatures. The last evidences that, after compacting at 6 GPa, all the samples acquire semiconducting properties so that behavior of  $\sigma(T)$  curves between 200 and 500 K denotes the state of “impurities depletion” due to their complete ionization when carrier transport is determined only by temperature dependence of mobility (due to their scattering on phonons) because concentration of impurity carriers is constant (no changes with temperature). Let us note that very close behavior of  $\sigma(T)$  was observed in [8] for undoped  $\text{Ca}_3\text{Co}_4\text{O}_9$  and doped with Ag and Lu.

As follows from the above analysis, the ratio of thermal to electrical conductivity ( $\sigma/\lambda$ ) after compacting at high pressure increased twice that explains the increase of  $ZT$  also twice.

Linear progress of  $\alpha(T)$  curves in Fig. 2b testifies validity of the known Mott relation [9]:

$$\alpha(T) = \frac{c_e}{n} + \frac{\pi^2 k_B^2}{3e} \left[ \frac{\partial \ln g(\varepsilon)}{\partial \varepsilon} \right]_{\varepsilon=\varepsilon_F} \quad (3)$$

for the studied samples. Here  $c_e$  is specific heat of carriers,  $n$  — concentration of carriers,  $k_B$  — the Boltzmann constant,  $g(\varepsilon)$  — dependence of density of states on energy in the vicinity of Fermi level  $\varepsilon_F$ . The first contribution in (1), in accordance with [9], we can consider practically as constant and prevailing over the second one which is linearly dependent on temperature. Fitting  $\alpha(T)$  curves by linear dependences  $\alpha(T) = A + BT$  allowed us to estimate coefficients  $A = c_e/n$  and  $B = \frac{\pi^2 k_B^2}{3e} \left[ \frac{\partial \ln g(\varepsilon)}{\partial \varepsilon} \right]_{\varepsilon=\varepsilon_F}$  for all the samples studied. Calculations have confirmed the validity of the approach formulated in [9] for our samples showing actual permanence of carriers specific heat ratio to their concentration  $a = c_e/n$   $(1.10\text{--}1.25) \times 10^8$  V/K between 200 and 600 K. This correlates with the above mentioned behavior of  $\sigma(T)$  dependences in this temperature range due to depletion of impurities.

#### 4. Conclusion

It is shown that iron and yttrium doping of the studied ceramics  $\text{Ca}_3\text{Co}_4\text{O}_9$  does not alter their crystalline structure. Increasing the compacting pressure before the diffusion annealing leads to a smaller-grained structure and reducing of the synthesized samples porosity. The last results in the increase of  $\sigma/\lambda$  ratio and  $ZT$  values. The Seebeck coefficient of  $\text{Ca}_3\text{Co}_{3.9}\text{Fe}_{0.1}\text{O}_9$  and  $(\text{Ca}_{2.9}\text{Y}_{0.1})(\text{Co}_{3.9}\text{Fe}_{0.1})\text{O}_9$  samples is not changed after compacting pressure increase displaying linear dependences on temperature.

#### Acknowledgments

The authors would like to thank the Institute of Heat and Mass Exchange of NAS Belarus for possibility to make measurements of thermoelectric properties on automated measuring system. Dr. T.N. Koltunowicz is a participant of the project: “Qualifications for the labour market — employer friendly university”, cofinanced by European Union from European Social Fund.

#### References

- [1] S. Isobe, T. Tani, Y. Masuda, W.-S. Seo, K. Koumoto, *Jpn. J. Appl. Phys.* **41**, 731 (2002).
- [2] T. Fujii, I. Terasaki, in: *Proceedings ICT'02. Twenty-First Int. Conf. Thermoelectrics*, IEEE Publisher, Piscataway 2002, p. 199.
- [3] B. Fisher, L. Patlagan, G.M. Reisner, A. Knizhnik, *Phys. Rev. B* **61**, 470 (2000).
- [4] Y. Wang, Y. Sui, X. Wang, W. Su, X. Liu, *J. Appl. Phys.* **107**, 033708 (2010).
- [5] I.P. Zvyagin, *Phys. Status Solidi B* **58**, 443 (1973).
- [6] T.C. Harman, *J. Appl. Phys.* **29**, 1373 (1958).
- [7] A.F. Ioffe, *Semiconducting Thermoelements*, Academy of Sciences of USSR, Moscow 1956.
- [8] G. Yang, Q. Ramasse, R.F. Klie, *Phys. Rev.* **78**, 153109 (2008).
- [9] T. Takeuchi, T. Kondo, T. Takami, H. Takahashi, H. Ikuta, U. Mizutani, K. Soda, R. Funahashi, M. Shikano, M. Mikami, S. Tsuda, T. Yokoya, S. Shin, T. Muro, *Phys. Rev. B* **69**, 125410 (2004).